STUDIA UBB CHEMIA, LXVIII, 4, 2023 (p. 137-154)
(RECOMMENDED CITATION)
DOI:10.24193/subbchem.2023.4.10

KETOCONAZOLE-PAMAM DENDRIMER SUPRAMOLECULAR COMPLEX FOR PROLONGED DELIVERY BY IN VITRO AND IN VIVO STUDIES

Irina KACSO[a], Ioana BÂLDEA[b], Maria MICLĂUȘ[a], Augustin MOȚ[a,c], Remus MOLDOVAN[b], Flavia MARTIN[a,*]

ABSTRACT. The current study investigates the potential of the supramolecular complex between the antifungal agent Ketoconazole (KTZ) and PAMAM dendrimer G5 generation to be used as a topically applied antimycotic drug. The new drug-dendrimer formulation was confirmed by combining XRPD, FT-IR and DSC analytical techniques, and presents improved aqueous solubility and delayed in vitro release profile compare to pure KTZ. The biological assays data showed the biocompatibility of the supramolecular complex and improved delivery of the encapsulated KTZ into the superficial layers of skin and mucosa at the mycotic infections site, leading to a better outcome of the infection.

Keywords: *Ketoconazole, PAMAM dendrimer, Drug-dendrimer complex, Solubility, Cell viability, Mouse ear sensitization test*

INTRODUCTION

Invasive fungal infections are a major cause of morbidity and mortality in premature infants, immuno-compromised patients or in those with acquired immune deficiency syndrome [1, 2].

[a] *National Institute for R&D of Isotopic and Molecular Technologies, 67-103 Donat str., RO-400293 Cluj-Napoca, Romania*
[b] *Department of Physiology, Iuliu Haţieganu University of Medicine and Pharmacy, 1 Clinicilor str., RO-400006 Cluj-Napoca, Romania*
[c] *Department of Chemistry, Faculty of Chemistry and Chemical Engineering, 11 Arany Janos str., RO-400028 Cluj-Napoca, Romania*
* *Corresponding author: flavia.martin@itim-cj.ro*

Azole antifungal agents represent the most important class of drugs used in clinical treatment of fungal infections. **Ketoconazole** (**KTZ**, $C_{26}H_{28}Cl_2N_4O_4$, *cis*-1-acetyl-4-[4-[2-(2,4-dichlorophenyl)-2-(1H-imidazol-1-ylmethyl)-1,3-dioxolan-4-yl]methoxy]phenyl]piperazine, **Figure 1**) was the first broad-spectrum oral antifungal Active Pharmaceutical Ingredient (API) approved by U.S. Food and Drug Administration (FDA) in 1981.

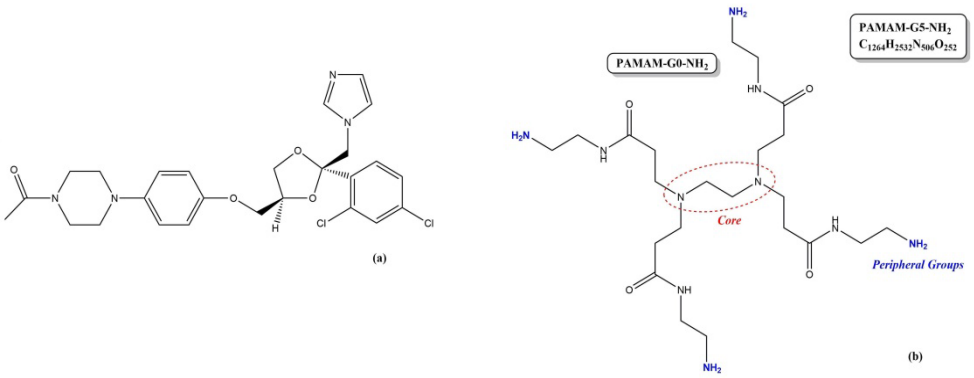

Figure 1. Chemical structure of **Ketoconazole (KTZ)** (a) and polyamidoamine dendrimer of G5 generation **(PAMAM-G5-NH_2)** (b)

According to Biopharmaceutics Classification System, **KTZ** is a class II drug, with low solubility and high permeability [3]. It's very low aqueous solubility, 0.017 mg/mL [4], limits its bioavailability, because the drug is eliminated from the gastrointestinal tract before it is completely dissolved, reducing its absorption into the blood circulation. Despite post-marketing reports of drug-related hepatotoxicity, it's been used, off-label, as a second-line therapy for castration-resistant prostate cancer [5], and in 2014 the European Medicines Agency approved *Ketoconazole HRA* for oral use as a second-line drug in Cushing's disease [6]. Because poor systemic absorption was observed from topical formulations, **KTZ** is often used for dermatological conditions [7].

In order to enhance the solubility and bioavailability of **KTZ,** different solid forms, salts or cocrystals, obtained by *crystal engineering* approach and using different co-formers, *e.g.*, dicarboxylic acids [8, 9], *p*-amino-benzoic acid [10], some phenolic acids [11], have been reported. Another way for its solubility enhancement is based on *formulations*, as solid dispersions [12], hot-melt extrusion [13] or inclusion complexes with beta-cyclodextrins [14].

The ability of *dendrimers* to encapsulate and form complexes with drugs and biologically active products rely on their unique properties, such as hyperbranching, well-defined spherical structure, and high compatibility with the

biological systems [15-17]. One of the most-studied starburst macromolecules is represented by *PAMAM (polyamidoamine) dendrimers*, their specific properties and low toxicity make them suitable as drug delivery systems and with the ability of controlled drug release [18, 19]. **KTZ** pharmaceutical formulations based on PAMAM dendrimers were also reported. Two studies have evaluated the **KTZ** solubility in the presence of PAMAM-NH_2 dendrimers of G1-G3 low generations, in hydrogel [20] and in solution forms [21].

The aim of this study is to evaluate the potential of the PAMAM dendrimer of higher generation, G5, with amine peripheral groups to encapsulate and to act as a carrier for the antifungal agent **KTZ** for topical therapy of cutaneous mycosis. The encapsulation is performed by the lyophilization method, a simple and reproductible one, often used for preparing this type of formulations. The physico-chemical and performance attributes of the new **KTZ-PAMAM-G5-NH_2** supramolecular complex were investigated by various thermo-analytical and spectroscopic techniques. The biocompatibility was assessed on normal dermal fibroblasts and hepatic cell line HepG2 and the risk for allergy induction following cutaneous exposure with the KTZ-dendrimer formulation was tested by the mouse ear swelling test.

RESULTS AND DISCUSSION

Generally, high generation PAMAM dendrimers possesses high-density amino groups on the surface with positive charge, while low generation PAMAMs contain a reduced and incompact peripheral structure. The interaction between the selected dendrimer, **PAMAM-G5-NH_2**, and the active substance **KTZ** is of host-guest type (e.g., electrostatic interactions, hydrogen bonds) and consist in simple encapsulation of the API in dendrimer cavities [22]. The physical entrapment approach of guest molecules into dendrimer cavity is usually performed in a single stage, as compared to the chemical conjugation method, which requires multiple stages [23, 24].

1. Identification of the supramolecular complex

Powder X-ray Diffraction

The powder X-ray diffraction (PXRD) patterns of the pure **KTZ** [8] and the lyophilized **KTZ-PAMAM-G5-NH_2** supramolecular complex are shown in **Figure 2**.

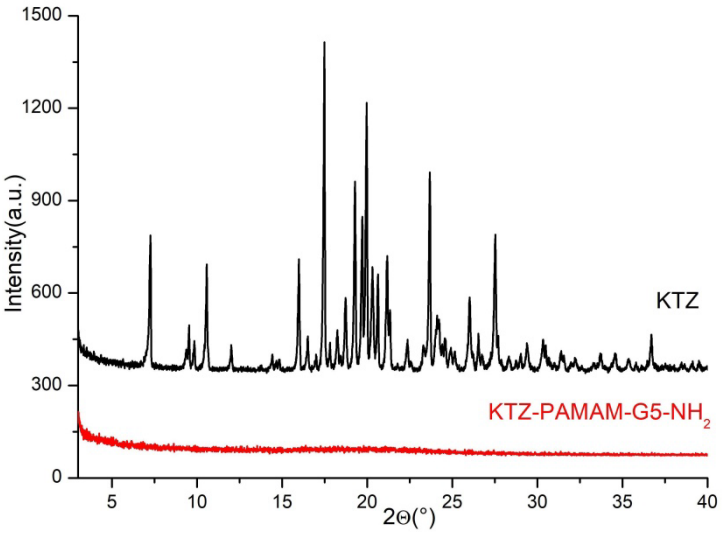

Figure 2. Experimental PXRD patterns of the **KTZ** and **KTZ-PAMAM-G5-NH$_2$** supramolecular complex

The powder diffraction pattern of the supramolecular complex displays an amorphous structure, characterized by long-range ordering. Thus, the disappearance of all the characteristic diffraction lines of **KTZ** is observed, proving its encapsulation in the cavity of **PAMAM-G5-NH$_2$** dendrimer.

FT-IR spectroscopy analysis

FT-IR was used to study the interaction between **KTZ** and **PAMAM-G5-NH$_2$** dendrimer, and the structural changes in the complex compared to free dendrimer. FT-IR spectra of the pure **KTZ**, **PAMAM-G5-NH$_2$** dendrimer and **KTZ-PAMAM-G5-NH$_2$** supramolecular complex are exposed in **Figure 3**.

In the FT-IR absorption spectra of the supramolecular complex the characteristic bands of the two components, **KTZ** [25, 26] and **PAMAM-G5-NH$_2$** dendrimer [27] can be identified with their slight modifications, consisting in the broadening of the bands and the displacement of the maxima of some bands or even the absence of others, due to compounds interactions and amorphous character of the supramolecular complex. Compared to the FT-IR spectrum of pure **KTZ**, one can observe: the characteristic bands of the stretching vibrations of the -NH groups at 3118 cm^{-1} and 2883 cm^{-1} are not found on the supramolecular complex spectrum, the weak intensity stretching vibration of the C=O carbonyl group from 1726 cm^{-1} shifts and appears as a weak shoulder of the amide band of dendrimer at 1743 cm^{-1}, the vibrational band

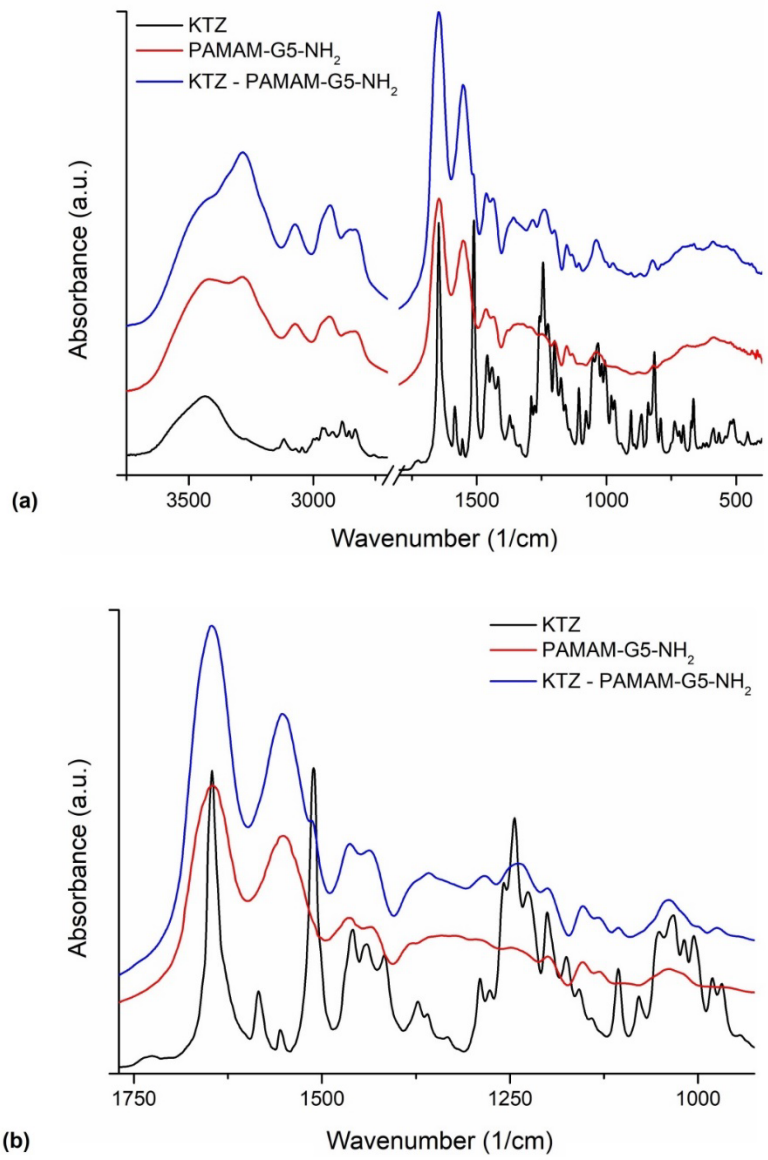

Figure 3. FT-IR spectra of **KTZ**, **PAMAM-G5-NH$_2$** and **KTZ-PAMAM-G5-NH$_2$** in the 3750–500 cm^{-1} (a) and 1770-925 cm^{-1} (b) spectral domain

of KTZ from 1510 cm^{-1} shifts and appears as a shoulder at 1514 cm^{-1} and the bands from 1373 cm^{-1} and 1360 cm^{-1} are shifted and appear as a broad band with a shoulder at 1378 cm^{-1} and the maximum at 1358 cm^{-1}; the vibrational

bands located at 1258, 1244 and 1223 cm^{-1} appear as a broad band with a maximum at 1237 cm^{-1}. The vibrational bands of the C-Cl bond appear as broad bands or shoulders, being shifted from 1006, 826, and 822 cm^{-1} to 1000, 737, and 733 cm^{-1}, respectively. Regarding the occurred changes in the spectrum of the dendrimer after complexation, one can observed the shift of the vibration bands from 1644, 1435 and 1250 cm^{-1} at 1647, 1437 and 1238 cm^{-1}, respectively. The resulting changes are due to weak interactions (electrostatic interactions, hydrogen bonds), which are formed between the two components.

Differential Scanning Calorimetry thermal analysis

The thermal behavior of the supramolecular complex is illustrated by the DSC curve in the temperature range 20-250 ºC (**Figure 4**). Several endothermic signals appear, among which can be identified: the broad peak of dendrimer **PAMAM-G5-NH$_2$** from 118.9 ºC moved to 114.8 ºC; a sharp endothermic signal with a maximum at 117 ºC; the melting signal of **KTZ** at 149.5 ºC appears as a broad low-intensity peak with a maximum at 146.9 ºC.

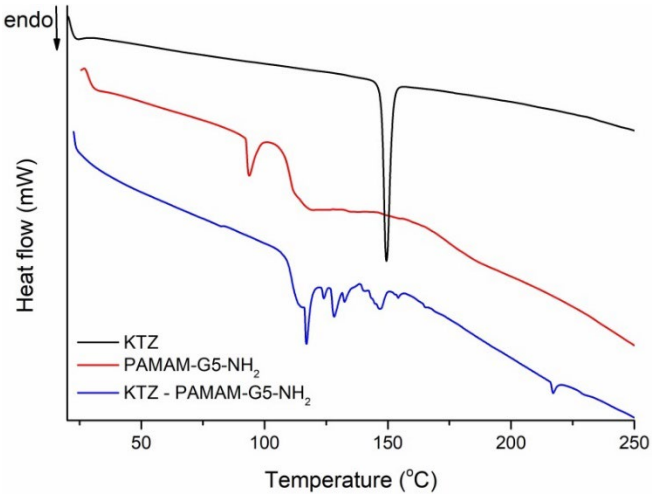

Figure 4. DSC traces of **KTZ**, **PAMAM-G5-NH$_2$** and **KTZ-PAMAM-G5-NH$_2$**

The differences identified on DSC curve of the supramolecular complex compared to DSC curves of the starting substances **KTZ** and **PAMAM-G5-NH$_2$** denote the presence of weak interactions between them with the formation of a material with a high degree of amorphous content, as determined already by XRPD, and different thermal events compared to the starting components.

2. Aqueous solubility of supramolecular complex

The evolution of the dissolution process over time in aqueous systems is an indicative of how a solid form is absorbed into the body. The aqueous solubility of the **KTZ-PAMAM-G5-NH$_2$** supramolecular complex was investigated using the optical nephelometric method [28]. This analytical technique involves measuring the degree of relative turbidity, due to the diffusion or scattering of monochromatic light, as Tyndall effect, caused by the insoluble particles dispersed in the solution. **Figure 5** and **6** show the scattered light spectra in the 500 – 700 nm spectral domain, for both **KTZ** and **KTZ-PAMAM-G5-NH$_2$** complex solutions, at different concentrations.

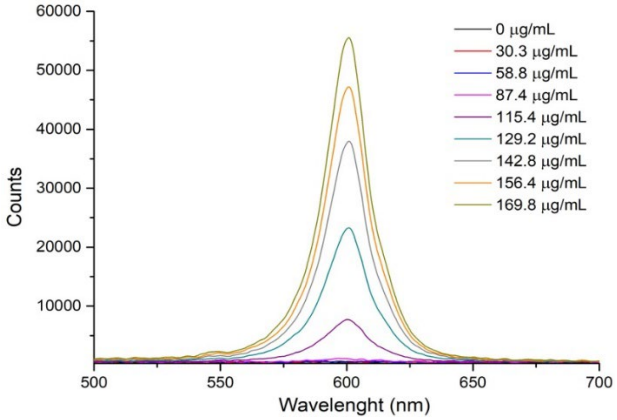

Figure 5. Spectra of scattered light for **KTZ** solutions at increasing concentrations

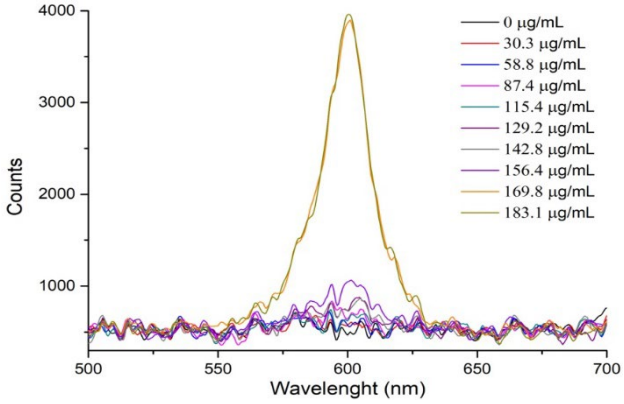

Figure 6. Spectra of scattered light for **KTZ-PAMAM-G5-NH$_2$** solutions at increasing concentrations

The aqueous solubility of pure **KTZ** and the **KTZ**-dendrimer formulation can be evaluated from the diffuse light intensity profile as a function of the concentration of the tested compound, as illustrated in **Figure 7**.

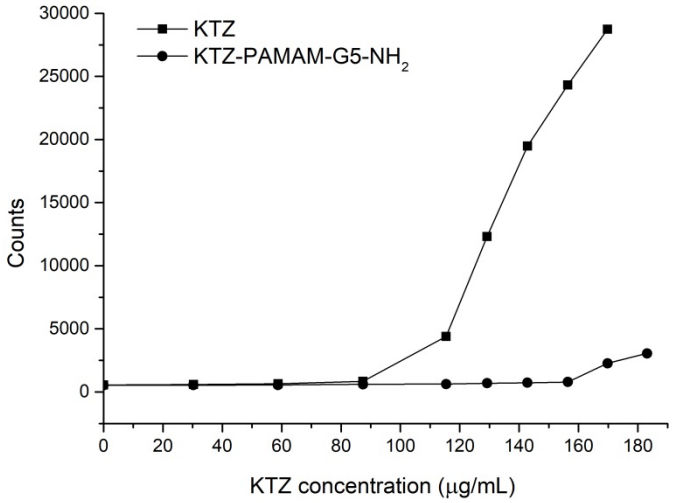

Figure 7. Evaluation of the limit solubility of **KTZ** and **KTZ-PAMAM-G5-NH$_2$** tested samples, from the variation of the diffuse radiation intensity at λ=590 nm depending on the concentration, in double-distilled water

In the case of the pure active substance **KTZ**, the solubility limit is detected by a sudden increase in the amount of suspended particles in double-distilled water at a concentration of 87.4 μg/mL.

On the other hand, the solubility limit for the supramolecular complex is detected at 156.5 μg/mL, but the precipitation process is very slow compared to that detected for **KTZ**. Thus, the encapsulated molecules of **KTZ** in the dendrimer cavity, through non-covalent bonds, are slowly released, so the solid particles will accumulate and finally precipitate in the aqueous solution.

3. In-vitro release profile of KTZ from the dendrimer supramolecular complex by the dialysis method

The stability of supramolecular complex and the encapsulation propensity of the **PAMAM-G5-NH$_2$** dendrimer were investigated by *the dialysis method* against double-distilled water [29, 30]. The *in vitro* release profile of pure **KTZ** and the **KTZ** encapsulated in the PAMAM dendrimer cavity was monitored by UV-Vis spectrophotometry (**Figure 8**).

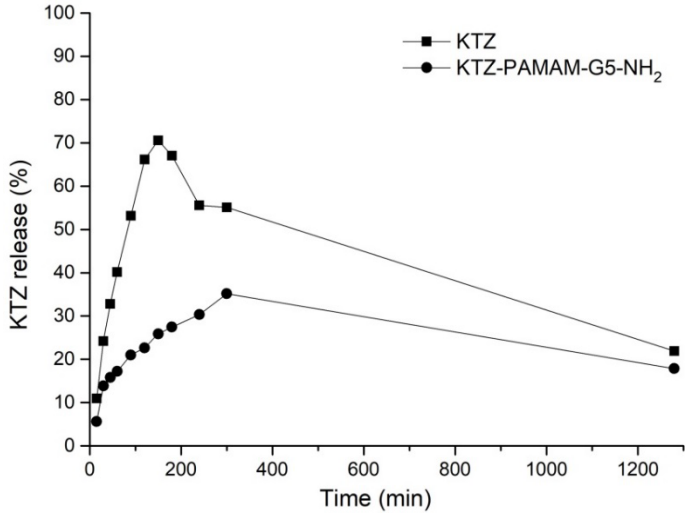

Figure 8. *In vitro* release of **KTZ** in **PAMAM-G5-NH$_2$** dendrimer aqueous solution compared with the pure **KTZ** release behavior

In the dialysis *in vitro* release experiment for pure **KTZ** during 150 minutes about 70% of the total amount of the active substance was released in the external aqueous phase, but, after 180 minutes, a decrease to 67% of the amount of KTZ was observed. This decrease in the amount of dissolved **KTZ** is due to the precipitation of the active substance in the external aqueous solution.

On the other hand, in the case of the **KTZ-PAMAM-G5-NH$_2$** complex, a slow release of the encapsulated drug was observed, thus after 90 minutes only ~20% of the amount of **KTZ** was released, and after 5 hours about 36%. Therefore, a continuous and considerably slower process of the **KTZ** released from the complex compared to pure **KTZ** occurred, without precipitation of the active substance in the external solution during the first 5 hours of the experiment. The *in vitro* release profile of **KTZ** from the dendrimer complex shows a controlled process vs. pure **KTZ,** probably due to its hydrophobic character, which allows it to remain longer embedded in the dendrimer cavities, suggesting that electrostatic interactions play an important role in drug release from dendritic complexes [21]. Our results are comparable to those reported for Ketoconazole- dendrimers PAMAM-G1-G3-NH$_2$ solution or hydrogel formulations [20, 21], but the *in vitro* release experiments were carried out in different conditions, as acidic pH or hydrogel components, which potentiates the solubility of KTZ.

Cell viability

Fibroblasts. Cell viability was reduced in a concentration-dependent manner in all treated groups. The concentration of 100 µg /mL decreased the cell viability below the toxic level of 70% in the case of **KTZ** and very close in the case of **PAMAM-G5-NH$_2$** and **KTZ-PAMAM-G5-NH$_2$**, respectively. These data confirm the toxicity of the compounds at a concentration greater than or equal to 100 µg/mL. Cells exposed to concentrations below 100 µg/mL demonstrated good viability. There are also no significant differences in viability between **KTZ** and **KTZ-PAMAM-G5-NH$_2$** treated groups at these concentrations (**Figure 9**).

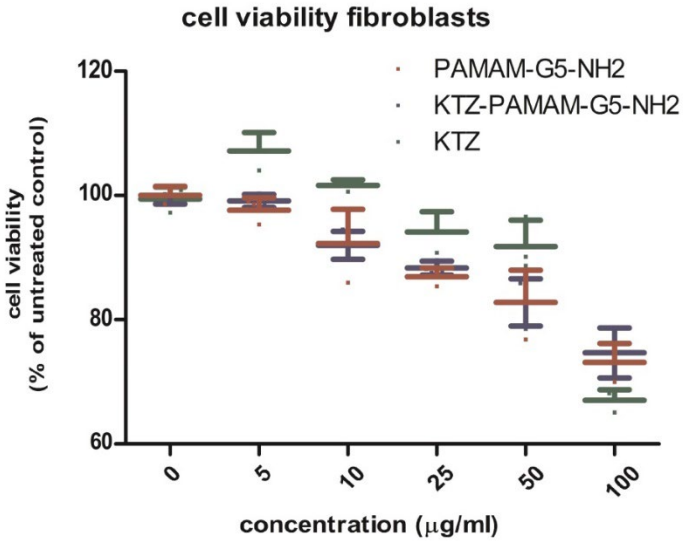

Figure 9. Cell viability of normal dermal fibroblasts (BJ) treated with **KTZ**, **PAMAM-G5-NH$_2$** dendrimer and **KTZ- PAMAM-G5-NH$_2$**, data are expressed as % of untreated controls.

Hep-G2. Cell viability was decreased in the **PAMAM-G5-NH$_2$** and **KTZ-PAMAM-G5-NH$_2$** groups in a dose-dependent manner but was maintained above the toxicity limit (70%) at concentrations below 200 µg/mL. **KTZ** did not cause a significant decrease in viability at all tested concentrations. These data confirm good liver cell viability at the **KTZ-PAMAM-G5-NH$_2$** complex up to a concentration of 100 µg/mL. In liver cells, **KTZ-PAMAM-G5-NH$_2$** showed toxicity at higher doses, compared to **KTZ** (**Figure 10**).

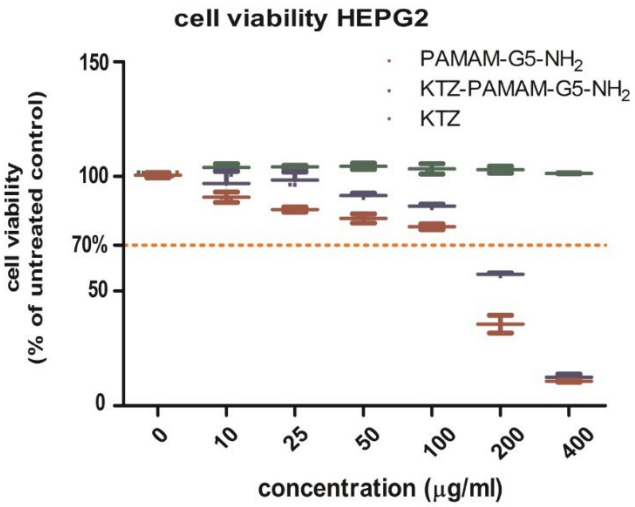

Figure 10. Cell viability of hepatic carcinoma cells (Hep-G2) treated with **KTZ**, **PAMAM-G5-NH₂** dendrimer and **KTZ- PAMAM-G5-NH₂**, data are expressed as % of untreated controls

4. Epicutaneous auricular sensitization test in mouse model

Mice were observed for any distress sign due to the cutaneous application of the substances. All mice survived and there was no weight loss, or hair loss during the exposure period. The mice in the dinitrochlorobenzene (DNCB) group showed swelling of the treated ear, as well as the tendency to scratch and at rechallenge, they showed signs of local pain-retraction of the head and vocalization, when the treated ear was touched, localized erythema, edema. All the other groups showed no macroscopic ear modifications at any of the measurement points (**Figure 11**).

Figure 11. Comparative images of BALB c mice ears treated with vehicle - negative control, DNCB - positive control and the test compounds: **KTZ**, **PAMAM-G5-NH₂** and **KTZ-PAMAM-G5-NH₂**

The obtained data from the MEST show a statistically significant increase in ear thickness in the DNCB group, the positive control group, which confirms the validity of the test model. In the other groups, no significant differences were obtained compared to vehicle-control, at any of the time points when measurements were made (**Figure 12**). Therefore, data show the validity of the model with epicutaneous sensitization in the positive control-DNCB group and no sensitization following exposure to the **KTZ**, **PAMAM-G5-NH$_2$** and respectively **KTZ- PAMAM-G5-NH$_2$**.

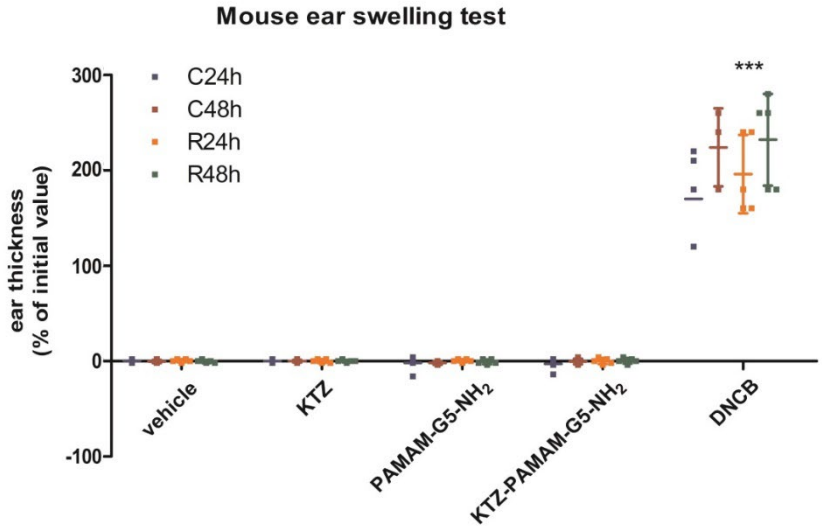

Figure 12. Epicutaneous mouse ear sensitization test using 5 experimental groups (n=5animals/group): control – vehicle, positive control - DNCB, and the test compounds: **KTZ**, **PAMAM-G5-NH$_2$**, and **KTZ-PAMAM-G5-NH$_2$** (***= p<0,0001)

Ear thickness measurements for each group after challenge at 24h (C24h), challenge at 48h (C48h) and respectively rechallenge at 24h (R24h) and 48h (R48h) are presented as % of initial ear thickness as media± standard deviation.

Cell viability tests proved that **KTZ-PAMAM-G5-NH$_2$** was well tolerated by the skin cells, dermal fibroblasts, in concentrations bellow 100 µg/mL and very well by the hepatic carcinoma cells, at concentrations up to 400 µg/mL.

CONCLUSIONS

Drug-dendrimer complexation is a widely used approach in pharmaceutical industries to increase stability, solubility, bioavailability and controlled release of drugs.

The current study evaluated the potential of the **PAMAM-G5-NH_2** dendrimer as drug carrier for the active antifungal **KTZ**. Being a BCS class II drug, its very low aqueous solubility represents a major disadvantage for its efficacy. Therefore, an increase of its solubility/bioavailability would lower the dose required for the therapeutic effect, and at the same time, provide hepatoprotection.

The new drug-dendrimer based formulation, obtained through non-covalent bonds, was confirmed by combining XRPD, FT-IR, DSC techniques. The supramolecular complex presents improved aqueous solubility over pure **KTZ**, and the *in vitro* release profile exhibited the delayed release of the encapsulated **KTZ,** being also achieved in a controlled manner compared to pure API. The biological assays data showed the biocompatibility of the tested compound and are encouraging for the potential application of the **KTZ-PAMAM-G5-NH_2** supramolecular complex in topical therapy of cutaneous mycosis. **KTZ-PAMAM-G5-NH_2** can improve the delivery of **KTZ** into the superficial layers of the skin and mucosa, at the mycotic infections site, due to their better stability, leading to a better outcome of the infection. However, more studies are needed to prove the bioavailability and the enhancement of the antimycotic properties, which will be addressed in future research.

EXPERIMENTAL SECTION

Materials

Ketoconazole, commercial form, was purchased from Melone Pharmaceutical Co. Ltd., China, and used without further purification. Amine-terminated fifth-generation PAMAM (polyamidoamine) dendrimer with ethylenediamine core (molecular weight = 28824.81 g/mol, 128 amine end groups) as 5% methanolic solution was purchased from Sigma-Aldrich Chemical Company, USA. Reagent grade solvents were purchased from Merk. Balc c mouse model were purchased from Cantacuzino Institute, Bucharest, Romania. All lab animal experiments were approved by ethics committee of the University of Medicine and Pharmacy Cluj-Napoca and the Veterinary Health Directorate, Romania (authorization number 329 / 17 08 2022).

Encapsulation of Ketoconazol in PAMAM-G5-NH_2 dendrimer

20 mg KTZ was dissolved in 1 mL methanol and magnetically stirred for 30 min at room temperature, following which 1.36 mL methanolic solution of **PAMAM-G5-NH_2** was added (**KTZ:PAMAM-G5-NH_2** = 10:1 molar ratio). The reaction mixture was stirred for 24h in the dark, then lyophilized for 24h to remove methanol. The **KTZ-PAMAM-G5-NH_2** supramolecular complex was obtained in the form of translucent sticky clay. The solvent removal was performed with an Alpha 1-2 LD type freeze dryer, at -55 °C and 0.010 atm.

Powder X-ray Diffraction

X-ray patterns were collected at room temperature using a Rigaku SmartLab multipurpose diffractometer, with Cu Kα1 radiation (λ = 1.54056 Å), equipped with a 9 kW rotating anode. For the acquisition of the experimental data, Smart- Lab Guidance software was used. The samples were ground to a fine homogeneous powder using an agate pestle and mortar and mounted on a sample holder. The measurements were performed in the 3°–40° 2θ range using steps of 0.01°.

FT-IR spectroscopy analysis

FT-IR spectra were obtained with a resolution of 4 cm^{-1} using a JASCO 6100 FT-IR spectrometer in the 4000–400 cm^{-1} spectral domain by employing the KBr pellet technique. Each sample has been dispersed in about 300 mg of anhydrous KBr, and the resulting powder was ground in an agate mortar. The pellet was obtained by pressing the ground mixture into an evacuated die. The spectra were collected and analysed with Jasco Spectra Manager v.2 software.

Differential Scanning Calorimetry analysis

Thermal measurements were performed with a DSC-60 Shimadzu differential scanning calorimeter and a SDT Q600 TA Instruments thermogravimeter. For the DSC measurements, standard aluminum crimped pan was used as sample holder and alumina as reference sample. An amount about 1.5–1.7 mg of each sample has been analysed in the 20–300 °C temperature range under dry nitrogen flow (3.5 L h^{-1}) with a 10 °C min^{-1} heating rate. Each measurement was performed in triplicate. For data collection and analysis, the Shimadzu TA-WS60 and TA60 2.1 software were employed. The DSC calorimeter was calibrated with reference standards of zinc and indium.

Aqueous solubility evaluation by Nephelometric method

The experimental device is equipped with a Silver Nova CCD simultaneous detector, and the experiments were performed using an LED with a wavelength of λ=590 nm, and the integration time was set to 500 ms. The solubility test was performed in double-distilled water at room temperature and the stock solutions of substances **KTZ**, **PAMAM-G5-NH$_2$** dendrimer and **KTZ-PAMAM-G5-NH$_2$** supramolecular complex were prepared in DMSO. For each analyzed sample, the diffuse radiation spectrum was measured, for a series of solutions at increasing concentrations in 30 – 185 μg/mL range. Analytical samples were prepared by adding increasing volumes (5 – 10 μL) of the stock solution, in a volume of 1 mL double-distilled water.

In-vitro release profile of KTZ from the supramolecular complex by the dialysis method

The *in-vitro* release study consisted of the following steps: (i) methanolic solutions of pure **KTZ** and supramolecular complex **KTZ-PAMAM-G5-NH$_2$** (concentration 2 mg/mL relative to **KTZ**) are transferred to cellulose dialysis bags (MCO=14000 Da, Sigma Aldrich); (ii) dialysis bags are placed in beakers, each containing 40 mL double-distilled water, under magnetic stirring at room temperature; (iii) samples of 1 mL each are collected from the external aqueous phase at different time intervals (15 min ÷ 24 h), supplementing the external phase with 1 mL double-distilled water at each extraction; (iv) the accumulation of **KTZ** in the external aqueous phase by diffusion from the dialysis bags was followed by measuring the absorbance at 230 nm. Previously, the calibration curve was drawn using dilutions of known concentrations of **KTZ** stock solution (0.19 mM in H_2O:CH_3OH 1:1 (v:v)).

UV-VIS Spectrophotometer Jasco V-750, (Able Jasco, Japan) was used to estimate the amount of drug incorporated in the dendrimer, with characteristics: wavelength range: 160-900 nm, speed of variable scanning between 10 ÷ 4000 nm/min, scanning speed at spectral preview of 8000 nm/min. The measurements were made in quartz cells, using H_2O:CH_3OH 1:1 (v:v) mixture, solvents of analytical purity, as internal standard.

Cell viability

Cytotoxicity of the **KTZ**, **PAMAM-G5-NH$_2$** dendrimer, and **KTZ-PAMAM-G5-NH$_2$** supramolecular complex was tested on two human cell lines: human dermal fibroblasts (BJ, ATCC CRL-2522™Manassas, Virginia, USA) and hepatocellular carcinoma (HepG2-HB-8065, ATCC). Cells were maintained in DMEM (Dulbecco's Modified Eagle Medium) with high glucose, supplemented

with 5% fetal calf serum and penicillin/streptomycin, amphotericin (all purchased from Biochrome AG, Berlin, Germany), in standard culture conditions, medium was changed twice a week.

All compounds were dissolved in DMSO to make a stock solution of 10 mg/mL, and then the solutions were further diluted with medium to reach the final concentrations, used to treat the cells. Final DMSO concentration was <0.5%, nontoxic to the cells. Briefly, 104cells/well were seeded for 24h on 96 well plaques, and then exposed to increasing concentrations of each of the tested compounds 0-100 µg/mL for the dermal fibroblasts and respectively 0-400 µg/mL for the Hep-G2 cells. Cell viability of the cells was assessed by using CellTiter 96® AQueous Non-Radioactive Cell Proliferation Assay (Promega Corporation, Madison, USA), as indicated by the producer, measurement was done at 540 nm. Each experiment was done in triplicate, and the results are expressed as % of untreated control [10].

Epicutaneous auricular sensitization test in mouse model

The epicutaneous auricular sensitization test on an animal model (MEST- mouse ear sensitization test) was performed on the Balc C mouse model, females, 3 months old, average weight 21 g±3g. The animals were purchased from Cantacuzino Institute, (Bucharest, Romania). During the experiments, the animals were kept at humidity 65%, 21 °C, day/night cycles of 12 h, fed with standard food and water ad libitum. The food of the animals was supplemented with vitamin A (250UI/g) to enhance the sensitivity of the epicutaneous sensitization test.

The mice were divided into 5 groups (n=5/group): control – vehicle, 70% ethanol; positive control – 200 µg/mL dinitrochlorobenzene (DNCB) dissolved in 70% ethanol; **KTZ** – 100 µg/mL, dissolved in 70% ethanol; **PAMAM-G5-NH_2** – 100 µg/ml, dissolved in 70% ethanol; **KTZ-PAMAM-G5-NH_2** – 100 µg/mL, dissolved in 70% ethanol. On the first day, Freund's adjuvant (Sigma Aldrich) was injected into the right flank, subcutaneously, to stimulate the allergic response to the test substances [31, 32].

Skin sensitization was performed on the shaved abdominal skin by daily topical application of 100 µL solution for 6 days, followed by the application of 50 µl solution on the right ear on day 8 (challenge=C) and day 15 (rechallenge=R). Ear thickness was measured with a digital caliper before application of the solution (day 8 - initial thickness) and subsequently after each application at 24h (C24h, respectively R24h) and 48h (C48h, respectively R48h). The calculation was made according to the formula: % ear thickness = 100*(A-B)/B, A = ear thickness after treatment, B = initial ear thickness [31-35].

The mice were followed for signs of distress like loss of appetite, weight loss, hair loss, local pruritus and pain. Macroscopic pictures were taken to document the inflammatory changes in the mice ears.

Statistical analysis

The statistical interpretation of the obtained data was done using the program GraphPad Prism version 4.00 for Windows, Software, San Diego, CA, USA, the one-way ANOVA test, followed by Dunnet's multiple comparations posttest, $p<0.05$ was considered significant (www.graphpad.com).

ACKNOWLEDGMENTS

This research was funded by Romanian Ministry of Research, Innovation and Digitization - Executive Agency for Higher Education, Research, Development and Innovation Funding (UEFISCDI), project PN-III-P1-1.1-TE-2021-0244 and project PN 23 24 01 05.

REFERENCES

1. A. H. Groll; J. Lumb; *Future Microbiol*., **2012**, *7*, 179-184
2. D. T. Mlynarczyk; J. Dlugaszewska; A. Kaluzna-Mlynarczyk; T. Goslinski; *JCR*, **2021**, *330*, 599-617
3. G. L. Amidon; H. Lennernäs; V. P. Shah; J. R. Crison; *Pharm Res*., **1995**, *12(3*), 413-420
4. S. Basa; T. Muniyappan; P. Karatgi; R. Prabhu; R. Pillai; *Drug. Dev. Ind. Pharm*., **2008**, *34*, 1209-1218
5. E. N. Lo; L. A. Beckett; C. -X. Pan; D. Robles; J. M. Suga; J. M. Sands; P. N. Lara; *Prostate. Cancer. Prostatic. Dis*., **2015**, *18*, 144-148
6. European Medicines Agency. Ketoconazole HRA; http://www.ema.europa.eu/ema/index.jsp?curl=pages/medicines/human/medicines/003906/human_med_001814.jsp&mid=WC0b01ac058001d124
7. F. D. Choi; M. L. W. Juhasz; N. A. Mesinkovska; *J. Dermatolog. Treat*., 2019, *30(8)*, 760-771
8. F. A. Martin; M. M. Pop; G. Borodi; X. Filip; I. Kacso; *Cryst. Growth. Des.,* 2013, *13(10)*, 4295-4304
9. I. Kacso; L. M. Rus; F. Martin; M. Miclaus; X. Filip, M. Dan; *J. Therm. Anal. Calorim.,* **2021**, *143*, 3499-3506
10. F. Martin; M. Pop; I. Kacso; I. G. Grosu; M. Miclăuş; D. Vodnar; I. Lung; G. A. Filip; E. D. Olteanu; R. Moldovan; A. Nagy; X. Filip; I. Bâldea; *Molec. Pharmaceutics*, **2020**, *17(3)*, 919-932

11. X. Chen; D. Li; Z. Deng; H. Zhang; *Cryst. Growth Des*., **2020**, *20*, 6973-6982
12. A. K. Aggarwal; S. Jain; *Chem. Pharm. Bull.,* **2011**, *59*, 629-638
13. P. K. Mididoddi; M. A. Repka; *Eur. J. Pharm. Biopharm.,* **2007**, *66*, 95-105
14. J. Taraszewska; M. J. Kozbial; *Inclusion Phenom. Mol. Recognit. Chem*., **2005**, *53*, 155-161
15. A.S. Chauhan; *Molecules*, **2018**, *23(4)*, 938-947
16. A. Santos; F. Veiga; A. Figueiras; *Materials*, **2020**, *13(65)*, 1-31
17. V. Patel; P. Patel; J. V. Patel; P. M. Patel; *J. Indian Chem. Society*, **2022**, *99(7)*, 100516
18. N. P. Silva JR; F. P. Menacho; M. Chorilli; *J. Pharma.,* **2012**, *2*, 23-30
19. R.V. de Araújo; S. da Silva Santos; F. E. Igne; J. Giarolla; *Molecules*, **2018**, *23*, 2849-2876
20. K. Winnicka; M. Wroblewska; P. Wieczorek; P.T. Sacha; E. Tryniszewska; *Molecules,* **2012**, *17*, 4612-4624
21. J. Jose; R. N. Charyulu; *Optoelectronics and advanced materials – Rapid Communications*, **2016**, *10(7-8)*, 604–608
22. A. Chauhana; B. Antona; M. K. Singh; Dendrimers for drug solubilization, dissolution and bioavailability, *in Pharmaceutical Applications of Dendrimers*, A. Chauhan, H. Kulhari Eds.; Elsevier, **2019**, Chapter 3, pp. 59-92
23. B. Yavuz; S. B. Pehlivan; N. Unlu; *Sci. World J.,* **2013**, 732340
24. S. Svenson; *Chem. Soc. Rev*., **2015**, *44(12),* 4131-44
25. P. Papneja; M. Kumar Kataria; A. Bilandi; *EJPMR*, **2015**, *2(5),* 990-1014
26. A. Karolewicz; A. Górniak; E. Owczarek; A. Żurawska-Plaksej; J. Pluta Piwowar; *J. Therm. Anal. Calorim*., **2014**, *115,* 2487-2493
27. S. Uppuluri; P. R. Dvornic; J. W. Klimash; P. I. Carver; N. C. Beck Tan; The Properties of Dendritic Polymers I: Generation 5 Poly(amidoamine) Dendrimers, **2022**
28. C. D. Bevan; R. S. Lloyd; *Anal. Chem.*, **2000**, *72(8)*, 1781-1787
29. S. D'Souza; *Advances in Pharmaceutics*, **2014**, Art. ID 304757, 1-12
30. J. Jose; R. N. Charyulu; *Int. J. Pharm. Investig*., **2016**, *6(2)*, 123-127
31. J. -L. Garrigue; J. -F. Nicolas; R. Fraginals; C. Benezra; H. Bour; D. Schmitt; *Contact Dermatitis*., **1994**, *30(4)*, 231-237
32. P. S. Thorne; C. Hawk; S. D. Kaliszewski; P. D. Guiney; *Fundam. Appl. Tox.,* **1991**, *17*, 807-820
33. C. G. Shayne; J. D. Brendan; D. W. Dobbs, C. Reilly, R. D.Walsh, *Toxicol and Applied Pharmacol*, **1986**, *84:(1)*, 93-114
34. L. Tordesillas; R. Goswami; S. Benedé; G. Grishina; D. Dunkin; K. M. Järvinen; S. J. Maleki; H. A. Sampson; M. C. Berin; *J. Clin. Invest.* **2014**, *124(11)*, 4965-7
35. S. Danescu; G. A. Filip; R. Moldovan; D. Olteanu; A. Nagy; X. Filip; F. Martin; I. Kacso; I. Baldea; *Inflammopharmacology,* **2021**, *29(3)*, 721-733